ONLINE FIRST June 3, 2026

Engineering Transactions, **74**, https://doi.org/10.24423/engtrans.2025.3607
Institute of Fundamental Technological Research Polish Academy of Sciences (IPPT PAN)
Université de Lorraine • Poznan University of Technology

Research Paper

Non-Linear Analysis of Wrinkling Phenomena in Sandwich Beams with a Soft Core

Paweł Jasion[1)], Iwona Wstawska[1)*], Kamil Kołodziński[2)]

[1)] *Faculty of Mechanical Engineering*
[2)] *Faculty of Civil and Transport Engineering*

Poznan University of Technology
Poznań, Poland

*Corresponding Author: iwona.wstawska@put.poznan.pl

This work is devoted to the local stability analysis of sandwich beams with a light core. A linear as well as a non-linear numerical analysis is carried out with the use of the finite element method (FEM). Both material and geometrical nonlinearities are taken into account. The goal of the investigation is to examine the influence of the material model on the post-buckling behaviour of a sandwich beam, especially on the formation and development of wrinkles on the compressed face. A pure bending condition is considered for a beam simply supported at both ends. The results for materials of theoretical properties are presented as well as for data from experiments on aluminium sandwich beams. From the results, it is seen that the linear analysis of the wrinkling phenomenon for non-linear materials gives overestimated results and does not predict correctly the buckling shape.

Keywords: wrinkling, sandwich beams, bending, buckling, equilibrium path, non-linear analysis.

1. Introduction

The success in the design of a structure partially depends on the correct prediction, analytical or numerical, of the behaviour of this structure. Such a prediction is especially difficult when local phenomena play a fundamental role and when material properties are not uniform or change during the loading process. This is the case when sandwich structures are analysed, in which at least two substantially different materials are connected together, and a local loss of stability may appear in the form of short wrinkles.

The simplest approach to the stability analysis of sandwich structures is the application of methods that describe the problem in a linear way and that

allow determination of the buckling load value and buckling shape. The linear approach to wrinkling problems has been studied, e.g., by Douville and Le Grognec [26]. Various possible failure modes were presented, and the values of the critical load were obtained with the use of analytical solution and finite element method (FEM). The influence of geometry and material on the buckling behaviour of the beam was widely investigated. The wrinkling phenomenon, as a linear problem, has also been described analytically by Jasion and Magnucki [2, 5], where it was assumed that the buckling shape has the form of uniform waves distributed equally on the compressed face. A more realistic form consists of waves with maximum amplitude at the mid-length, which fade when moving towards the supports. An analytical approach to wrinkling of a compressed composite facing has been discussed by Birman and Bert [9], where the core was treated as an elastic foundation and various models of it were taken into the consideration. A novel analytical solution for buckling of sandwich panels/beams has been formulated by Cao and Niu [15]. The transverse shear deformation of the face sheet has also been considered. The face of the sandwich panel was modelled as a linearly elastic beam or plate. The authors stated that the faces should be considered as one beam made of many short ones, each having the length of one buckling wavelength, rather than a single slender beam.

Short wrinkles mentioned above may appear in sandwich structures with thin faces [1]. However, if the structure is rigid enough as a whole, global loss of stability may occur. Analytical investigation of both global and local behaviour of sandwich beams has been presented by Léotoing *et al.* [23]. The authors, based on analytical solution, provided design guidelines in the form of diagrams. Global buckling and wrinkling analyses of sandwich plates with anisotropic faces and an orthotropic core have been conducted by Vescovini *et al.* [13]. The critical loads as well as wrinkling modes were analysed for foam and honeycomb core materials subjected to uniaxial and multiaxial loads. A new model incorporating local instabilities and global buckling in sandwich structures has been proposed by Mhada and Bourihane [14]. The model was based on the technique of slowly varying Fourier coefficients. The main advantage of the presented model was obtaining results similar to those acquired with the use of other extended models, while decreasing computational time. The analysis of elastic buckling of isotropic, laminated composite and sandwich beams subjected to various loads and boundary conditions has been carried out by Karamanli and Aydogdu [16]. It was acknowledged that the type of applied load has a significant influence on the values of critical loads and mode shapes, which are also closely associated with boundary conditions. Global buckling was also considered by Jasion and Magnucki [3]. In the paper sandwich beams with aluminium facings and aluminium foam in the core were considered. Analytical solution of the stability problem was presented and compared with experimental data.

A linear analysis of a structure has some well-known disadvantages. One of them is the assumption of ideal geometrical deformation after buckling, which in the case of sandwich beams means regular waves on the upper face, a situation rarely possible due to different types of imperfections in actual structures. Another issue is that the materials used for the core are often some kind of foam and because of this they may behave in a non-linear way during deformation, which cannot be included in linear analysis. For this reason, non-linear analysis should be performed to analyse the behaviour of sandwich structures. A vast investigation of the behaviour of different materials used for cores has been considered by Lolive and Berthelot [11]. The comparison between the experiment and the numerical simulation for three-point bending was presented. The significance of experimental investigation in such problems was pointed out. The non-linear behaviour of a sandwich panel has been investigated by Frostig *et al.* [12]. The panel consisted of two faces, upper and lower, as well as a functionally graded core. The wrinkling and post-wrinkling response of the construction were taken into the consideration. The analysis confirmed that a functionally graded core can substantially improve the wrinkling stability of sandwich structures.

The complexity of the stability problem makes it necessary to use numerical methods, among which the most popular is FEM. Such an approach has been proposed by Sjölander *et al.* [7]. The authors analysed the case of forming composite laminates and showed that by changing the stacking sequence, wrinkles can be eliminated in certain locations. Moreover, special finite elements proper for modelling sandwich beams have been created and studied by Sudhakar *et al.* [8]. Furthermore, semi-analytical methods have been implemented by Liu *et al.* [17], who carried out a buckling analysis of functionally graded sandwich beams. The material properties of each layer were assumed to be graded along the thickness of the beams. The studies revealed that the boundary conditions have a meaningful influence on the buckling response of beams. In addition, the critical buckling loads increase with an increase in the constraints.

When local stability is analysed, geometrical imperfections of the face play a crucial role since they may initiate wrinkling or folding phenomena. The problem of imperfections in sandwich structures has been described by El-Sayed and Sridharan [10]. The wrinkling phenomenon in sandwich panels has been discussed by Fagerberg and Zenkert [25]. The importance of initial imperfections was pointed out, and the analytical model with such imperfections was provided. The comparison between analytical solution obtained from the model and the results of laboratory and numerical experiments showed the correctness of this approach.

The wrinkling phenomenon is still vividly examined and is not limited to classical sandwich structures. Stretching of soft shells with variable curvatures has been presented by Wang *et al.* [18]. Numerical analysis of the wrinkling be-

haviour of shell surfaces was performed, and phase diagrams defining stability boundaries were depicted. The analysis indicated that varying curvature suppress wrinkles and control the wrinkling and smoothing responses. Wrinkling analysis of circular membranes has been carried out by Huang *et al.* [22]. The instability mechanics of an annular membrane under in-plane stretching has also been investigated. Furthermore, the analysis of instability of a circular thin plate under in-plane compression was conducted. It was shown, in the case of an annular plate, that the value of Poisson's ratio and geometric dimensions have superior influence on wrinkling behaviour. In the case of a compressed plate, the wrinkling phenomenon is associated with boundary conditions.

A new method for predicting wrinkling stress in sandwich panels has been introduced and employed by Su and Liu [19]. The analysis showed that the values of wrinkling stress were highly dependent on the cell size of the foam core. Moreover, the values obtained with the use of this model were compared with those available in the literature. Good agreement was observed. An extensive study of critical and final wrinkling of thin-walled sheet/tube parts under various loading conditions has been carried out by Li *et al.* [20]. The authors revealed that wrinkling mostly occurs under a tension-compression stress state. The influence of material properties on wrinkling behaviour was not taken into the consideration because of variable loading conditions. The effect of wrinkles on the failure of flat laminates has been formulated by Hu *et al.* [21]. It was concluded that local stress concentrations around the wrinkles, as well as location of the wrinkles, play an important role in the failure mechanism of the examined laminates.

In actual structures, it is difficult to analyse the wrinkling problem since there may be some interaction between two or more materials, which may behave in a different way. When waves form on a beam, one or more materials may enter the plastic range and this may influence subsequent behaviour of the whole structure. In this work, the wrinkling phenomenon in sandwich beams is investigated numerically taking into account changes taking place in the material during deformation. The obtained results provide answers to questions that arise during the modelling of sandwich structures, while also helping to understand the wrinkling phenomenon and relating material properties to the buckling behaviour of the beam. First of all, it is shown how the elastic/plastic properties of the faces and core affect the post-buckling behaviour of a beam and influence the formation of wrinkles or dents. This knowledge can help in the design of sandwich structures with desired behaviour. Additionally, some knowledge concerning the buckling and limit loads for beams made of materials with different properties is provided. Finally, the comparison of finite element (FE) and experimental results confirms that a simplified 2D numerical model can accurately predict the behaviour of the actual structure. An exemplary paper devoted to

similar problem has been presented by STIFTINGER and RAMMERSTORFER [6], in which the influence of plastic properties of the core and the face on the post-buckling behaviour of sandwich beams under pure compression was presented. The post-buckling behaviour of sandwich beams has also been analysed by LÉOTOING *et al.* [24]. Here, the influence of the size of imperfection as well as core material properties on this behaviour was pointed out.

The content of the article is organised as follows. Section 2 presents details concerning the numerical modelling of the beam, including geometry and material. Section 3 contains the results of the analyses and begins with a brief description of the procedures used in the investigation. This is followed by four subsections in which first, the influence of mechanical properties of materials on the post-buckling behaviour of the beam is investigated, secondly, the behaviour of the upper face for different Young's moduli is described, thirdly, the influence of imperfection shape and magnitude on the post-buckling behaviour is analysed, and fourthly, the application of the proposed FE model to the analysis of an actual beam is presented. The last subsection also serves as a validation stage. Section 4 is the summary presenting the main conclusions.

2. Numerical model of the beam

2.1. Models of materials

The feature that distinguishes sandwich structures from other ones is that they combine two usually very different materials. The faces are made of tough solid material that carries most of the load, whereas the core is usually a very light filler in the form of a foam. The above fact suggests that special attention has to be paid when defining the model of material for numerical analysis. Moreover, the influence of this model on the behaviour of structure has to be carefully investigated.

Three different models of material are taken into account in this work. The first one is a linear elastic model shown in Fig. 1 with dashed lines. The simplicity

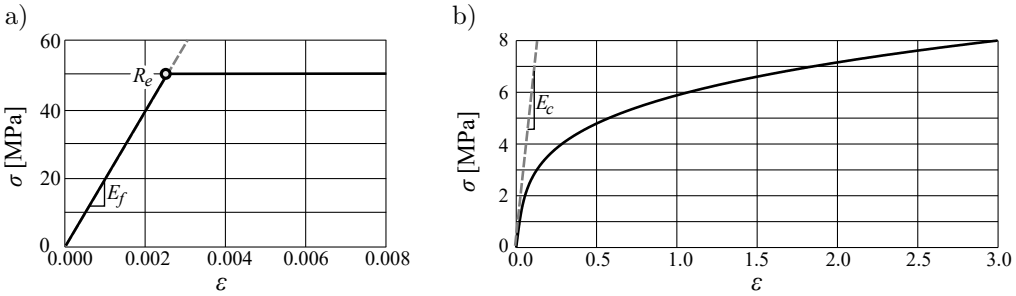

FIG. 1. Models of materials; linear elastic (dashed lines):
a) linear elastic-perfectly plastic, b) non-linear plastic.

of the model – the linear relationship between stress and strain – makes it very effective in numerical calculations. However, small strains assumed in this model are not applicable when the buckling phenomenon appears in a local range. Thus, when the mode of failure of the structure is to be analysed, a model that includes the plasticisation of material should be considered. The simplest approach is to choose an elastic-perfect plastic model. It assumes a linear stress-strain relationship up to the yield strength R_e and then the strains increase infinitely with a constant stress equal to R_e. Such a model is shown in Fig. 1a with a solid line.

The models described above are sufficient for materials such as steel or aluminium, which are often used as faces of sandwich structures. For manufacturing cores, lightweight materials such as foams made of plastic are used. Such materials may behave in a non-linear manner from the very beginning of loading process. Thus, in this case, a more proper model is a non-linear plastic one, shown in Fig. 1b with a solid line. Here, the stress-strain relationship is given by a series of points and described as

$$\varepsilon = \frac{\sigma}{E}\left[1 + c\left(\frac{\sigma}{E}\right)^{2m}\right], \tag{2.1}$$

where E is Young's modulus of the material at the beginning of the curve, and c and m are the constants determined based on experimental results. The shape of the curve is similar to that described by the classical formulae proposed by RAMBERG and OSGOOD [27].

Since the goal of this work is to investigate the influence of material properties, or in other words, the material model, on the behaviour of a beam, the mechanical properties of selected materials have been chosen to allow for the observation of all desired phenomena. For the material of the faces there are the following properties: $E_f = 20 \times 10^3$ MPa, $\nu = 0.3$, $R_e = 50$ MPa. The model of the core was prepared based on Eq. (2.1) with the following parameters: $E = 50$ MPa, $\nu = 0.3$, $c = 3000$, $m = 1.4$.

2.2. Model of the beam

All numerical calculations were performed with the use of ANSYS software. The following dimensions of the model were assumed: total length of the beam $L = 400$ mm, thickness of the face $t_f = 0.3$ mm, thickness of the core $t_c = 20$ mm, and width of the beam $b = 100$ mm. The total beam thickness equals $t = 20.6$ mm. Since wrinkling of the upper face is a local phenomenon, a dense finite element mesh is required to represent short wrinkles that may appear under pure bending conditions. Thus, it was decided to use a 2D model of the beam, shown in Fig. 2, with the assumption of a plane state of stress. Moreover, symmetry

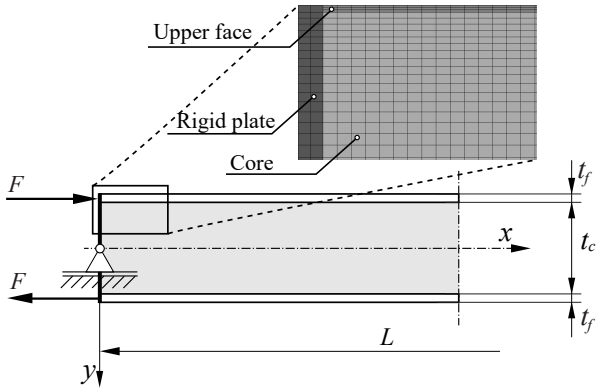

Fig. 2. FE model of the beam.

conditions were used at the mid-length of the beam, and consequently only half of the beam was modelled having in mind that with this approach only symmetrical deformation is possible. The preliminary research shows that the effective approach to model pure bending conditions is to connect all three layers to a rigid plate. The plate has a thickness of 1 mm and Young's modulus 10^3 times greater than the face's modulus. The load in the form of moment is achieved by applying normal forces F to the faces through the rigid plate – compressing force to the upper face and tensile force to the lower one, as it can be seen in Fig. 2.

The model is supported at the mid-height of the rigid plate. At the point of support, vertical movement is removed, while axial displacements are allowed. Such conditions define a movable pin support allowing the rigid end of the beam to move horizontally and rotate about the point of support. The displacement of the entire model is prevented by symmetry conditions at the mid-length.

Higher-order elements PLANE183 have been chosen with eight nodes and three degrees of freedom per node. A non-uniform mesh through the thickness of the core was applied starting from the mid-height of the core. The mesh was densified with the scaling factor of 4, which means that the FE near the upper face is four times thinner than the one at the mid-height of the core. Since the loss of stability has the form of short wrinkles distributed along the length of the beam, the most crucial parameter of the mesh is the number of elements along the axis, which was set to 350. The conducted convergency study showed that both increasing and decreasing this number change the critical load value by only a fraction of a percent. Two other analysed parameters, that is, the normal stress in the face and the maximum deflection of the beam, remain practically unchanged.

A similar convergency study was performed for the number of elements through the thickness of the upper face to prevent excessive stiffening due to

an insufficient number of elements. The obtained results revealed that, starting from only two elements through the thickness, the maximum deflection of the beam, maximum normal stress as well as the value of the critical moment are the same up to the fifth significant digit, regardless of the total number of elements. Bearing in mind that wrinkling is a local phenomenon, it was decided to use three elements rather than two through the thickness of the upper face in order to improve the representation of the actual beam behaviour in the model.

3. Results of studies

3.1. Procedures used in the analyses

Three types of analyses were conducted to investigate the behaviour of the beam during the whole loading process. First, a linear static analysis was performed to determine the stress distribution and to obtain input results for the next step, which was the linear buckling analysis. Here, the buckling loads, called critical moments, and the buckling shapes were determined. The first buckling mode served then as a geometry disturbance in the last, third type of analysis, namely the non-linear buckling one. This last step made it possible to include the non-linear behaviour of the material as well as geometrical imperfections into the model. As a result, equilibrium paths were derived, describing the post-buckling behaviour of the beam, including the limit load and the failure mode of the beam. The non-linear analyses were performed with the use of the arc-length method. The procedure available in the system makes it possible to follow the post-buckling behaviour of a structure, even in snap-through problems. The analysis was divided into 100 substeps, with 120 and 80 substeps as a possible maximum and minimum, respectively. The force convergence criterion was used to control the solution, which is a typical approach for the arc-length method. The available stabilisation option was turned off. A maximum displacement of the model, equal to 60 mm, was used as the criterion to stop the calculations.

3.2. Influence of mechanical properties of materials on the post-buckling behaviour of the beam

A typical buckling shape of a sandwich beam under pure bending has the form of short wrinkles in its upper part, as shown in Fig. 3a. Before wrinkles appear, the displacements are very small, and for many materials the process takes place in the elastic range. However, even for such small displacements, plastic strains may appear in a light core and this may influence the subsequent behaviour of the face. After buckling, plastic strains may appear also in stiff faces, since the deformation becomes much stronger. For these reasons, four different models of the beam with respect to materials will be considered.

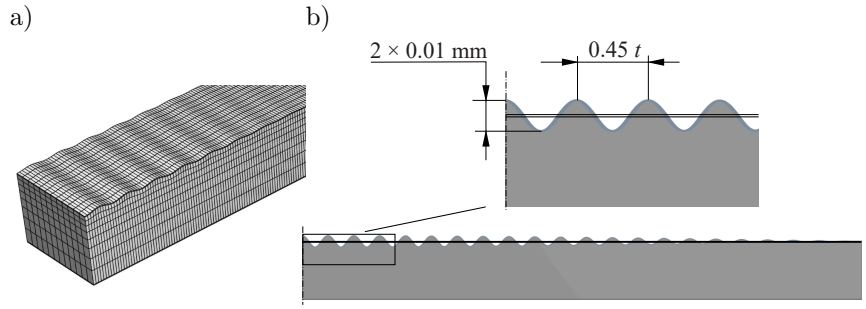

Fig. 3. Behaviour of the upper face of the bent beam: a) wrinkling phenomenon (exemplary FEM result), b) first eigenmode obtained from the linear buckling analysis, used as an imperfection pattern (increased scale).

All models are geometrically non-linear but differ in material formulation. The results of analyses are presented in the form of equilibrium paths; additionally, distributions of elastic or plastic strains, depending on material behaviour, are provided. The vertical axis of each path corresponds to the applied bending moment normalised by the critical moment; thus, a value equal to 1 corresponds to the buckling load, whereas the horizontal axis gives the value of displacement of the lower face measured at the mid-length of the beam. For the results presented in this subsection, geometrical imperfections in the form of the first eigenmode were used, which is a typical approach, at least at the initial stage of an investigation. According to Fig. 3b, these imperfections have the shape of a symmetrical fading sine wave with the maximum amplitude at the mid-length of the beam. Since the goal of the investigation is to analyse nearly perfect structures and to observe their response to different material properties, an amplitude of only 0.01 mm was used. The wavelength was approximately constant and equal to 0.45 of the total beam thickness. It should be noted that the number of waves results from the assumed mechanical properties of the materials and the geometry of the model.

In the first model, an elastic material model was ascribed to both the faces and the core. Two straight lines are visible on the equilibrium path (Fig. 4a). The first one, which is in the pre-buckling range, describes the linear behaviour of the structure. Here, the curvature of the beam increases, and the upper face remains plain with the exception of waves being the result of the initial geometrical imperfections. The second line describes the behaviour of the beam in the post-buckling range. The slope of this line, that is, the stiffness of the beam, is smaller due to the wrinkles on the upper face. The intersection of both lines, which can serve as an estimated buckling load, is about 3 % lower than the linear buckling load corresponding to unity on the vertical axis. As it can be seen in Fig. 4b, in which elastic strains are shown, just after the moment of buckling wrinkles appear at the mid-part of the beam over 2/3 of its length.

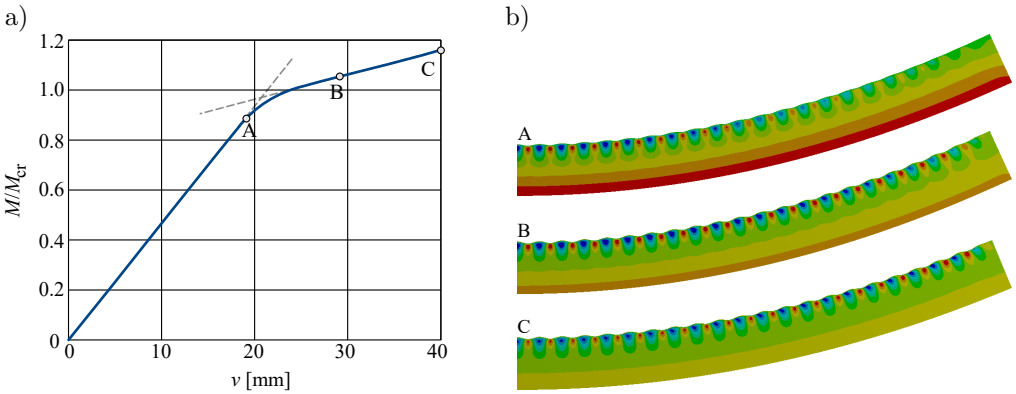

FIG. 4. Results of the post-buckling analysis of the beam with elastic faces and an elastic core: a) equilibrium path, b) distribution of elastic strain.

When the deflection increases, the wrinkles spread over the whole length of the structure. A further increase in deflection results in an increase in the amplitude of the wrinkles. It should be noted that the amplitude and the wavelength are the same along the entire beam.

In the second model of the beam, it is assumed that the core is made of a nonlinear material like the one described by the solid line in Fig. 1b. The material of the faces remains linear through the whole analysis. According to the equilibrium path shown in Fig. 5, initially, before point A, the wrinkles appear in the mid-part of the beam (image A in Fig. 5b). After that, the path bends sharply and then becomes almost horizontal, which indicates that the stiffness of the structure is very small. The reason is the formation of a single fold at the mid-length of the beam (image B in Fig. 5b). The amplitude of the other wrinkles diminishes. In the enlarged part of the plot, it is seen that, in the post-buckling

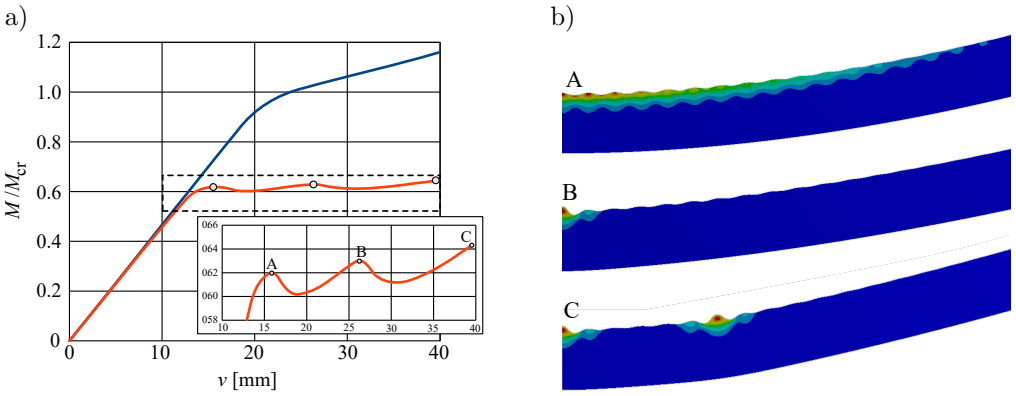

FIG. 5. Results of the post-buckling analysis of the beam with elastic faces and a plastic core: a) equilibrium path, b) distribution of plastic strain.

range, more peaks appear on the equilibrium path. The maximum of each corresponds to a change in the buckling mode, that is, to the start of formation of another single fold, as can be seen in image C in Fig. 5b. From the plot, it can be read that for this FE model, that is, with a plastic core, the buckling load is about 40 % smaller than that from the linear analysis. Since the plastic strains shown in Fig. 5b appear only in the core of the beam, the faces are not visible in the figure – they are transparent.

The third model consists of an elastic core and elastic-perfectly plastic faces. In this case, the buckling load drops considerably and constitutes only 22 % of the linear buckling load. As can be seen in Fig. 6a, after the loss of stability, the slope of the path sharply decreases and then remains approximately constant. The upper face deforms according to the imperfection shape. The size of wrinkles is very small, as can be seen in images A and B of Fig. 6b, even for large deflection of the beam. The distribution of elastic strains in the core at the final stage of the calculations is uniform.

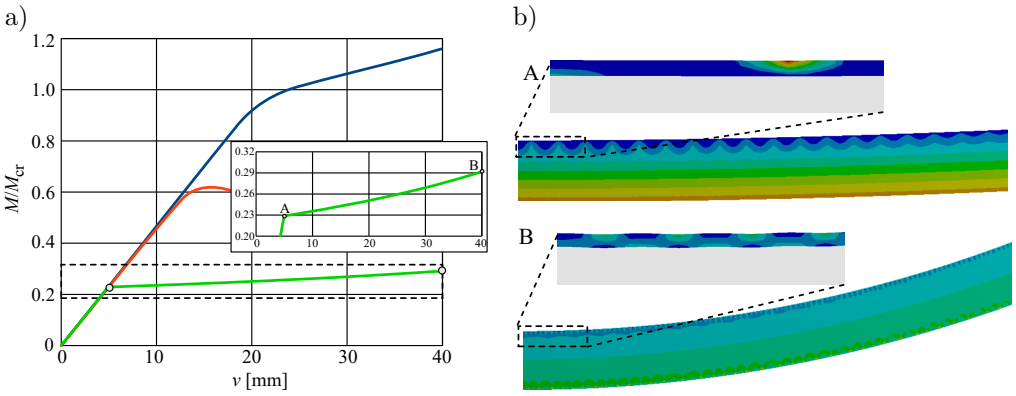

FIG. 6. Results of the post-buckling analysis of the beam with plastic faces and an elastic core: a) equilibrium path, b) distribution of elastic and plastic strain.

The fourth model analysed here is fully plastic. In this case, similarly to the previous case, the buckling load is only about 22 % of that obtained in the linear buckling analysis. The equilibrium path, shown in Fig. 7a, collapses sharply and then becomes horizontal. At the buckling load, a small plastic strain can be observed (Fig. 7b), with almost negligible wrinkles, and just after that point, one large fold directed inward forms near the mid-length of the beam. The enlarged part of the plots reveals that the formation of this fold is associated with a drop in the load up to some minimum, after which a small increase in the load is observed. In this model of the beam, both materials exhibit plastic behaviour, which can be observed in image B in Fig. 7b. Plastic strains are present in both the core and the faces.

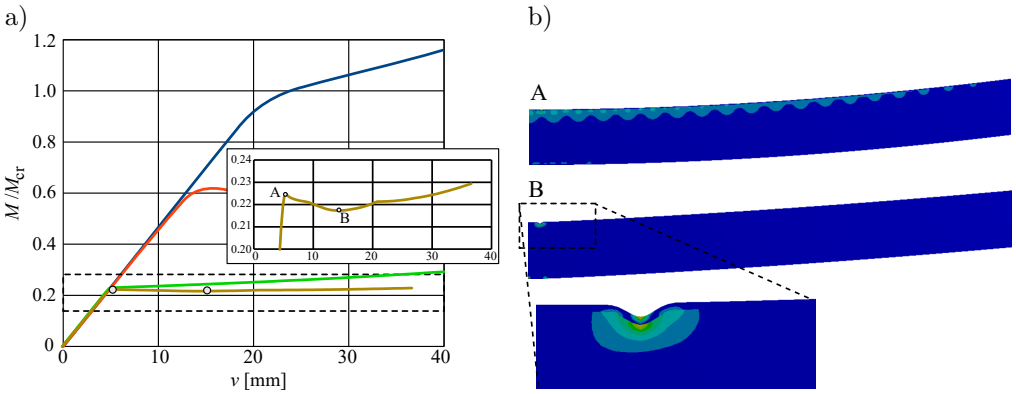

FIG. 7. Results of the post-buckling analysis of the beam with plastic faces and a plastic core: a) equilibrium path, b) distribution of plastic strain.

3.3. BEHAVIOUR OF THE UPPER FACE

Since the loss of stability of the sandwich beam depends on the behaviour of the upper face, it is reasonable to analyse the influence of the stiffness of this part as well as the foundation on which it rests, that is, the core, on the buckling behaviour of the whole structure. Since this study is focused on material properties, the stiffness will be modified by changing Young's modulus, while leaving the thickness of the face and the core unchanged. In the first group of models, the values of E_f will range from 1×10^3 MPa to 200×10^3 MPa, and E_c will remain unchanged and equal to 50 MPa. In the second group, the modulus of the face E_f equals 20×10^3 MPa and Young's modulus of the core E_c takes values equal to (10, 50, 100, 200, 300) MPa.

Let us start the considerations from the linear buckling analysis. As can be expected, the stiffness of the face influences the critical buckling load, which equals 20.3 Nm for $E_f = 1 \times 10^3$ MPa and 337.5 Nm for $E_f = 200 \times 10^3$ MPa. The mode of buckling is also different depending on Young's modulus. For lower values, a shorter wavelength is observed than for the highest analysed value, as can be seen in Fig. 8a. From the presented figures, it can be seen that the deformation of the core reaches much deeper when the stiffness of the face is higher.

When the stiffness of the core is considered to be variable, similar results are seen, that is, the higher Young's modulus, the higher the buckling load. In this case, the relationship is almost linear, as can be seen in Fig. 8b. The buckling shape is also influenced, but here the rise of stiffness increases the number of waves on the upper face.

More interesting information can be drawn when the same models of the beam are analysed with the use of a non-linear procedure. To observe the for-

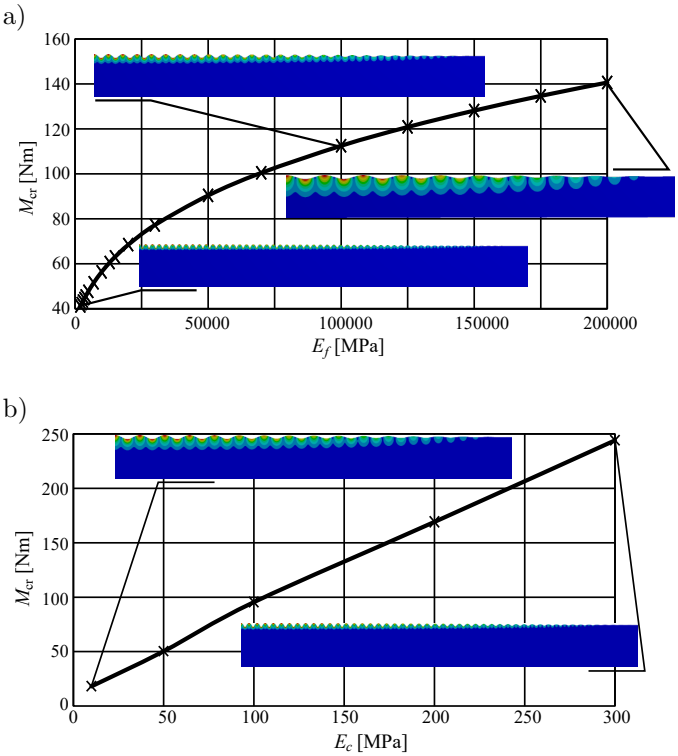

FIG. 8. Influence of Young's modulus of the face (a) and the core (b) on the critical load.

mation of wrinkles, the model of material of the faces is elastic, whereas the model for the core is a non-linear one and defined as in the previous analyses. The first thing that should be noted is the stiffness of the beam in the initial range of deformation, as indicated by the slope of the equilibrium paths shown in Fig. 9. When the absolute value of the load is taken into account, the stiffness of the beam, defined as the ratio of load to maximum deflection, increases from 0.2 for $E_f = 1 \times 10^3$ MPa to 30 for $E_f = 200 \times 10^3$ MPa, assuming that the stiffness of the core is the same for all models. Of course, the limit load also increases with the increase of E_f (see Fig. 9b). A different behaviour can be observed when Young's modulus of the core is variable. As can be seen in Fig. 9d, the stiffness of the beam is more or less constant and only the limit load increases with the increase of E_c.

Additional analysis of the obtained results is provided in Fig. 9a and Fig. 9c. In these plots, the vertical axis corresponds to the dimensionless load, that is, the applied moment divided by the critical moment being the results of the linear buckling analysis. Interestingly, the non-linear critical load for all models is similar and corresponds to about 62 % of the linear buckling load. In other words, regardless of the stiffness of the face, the critical load decreases by about 38 %.

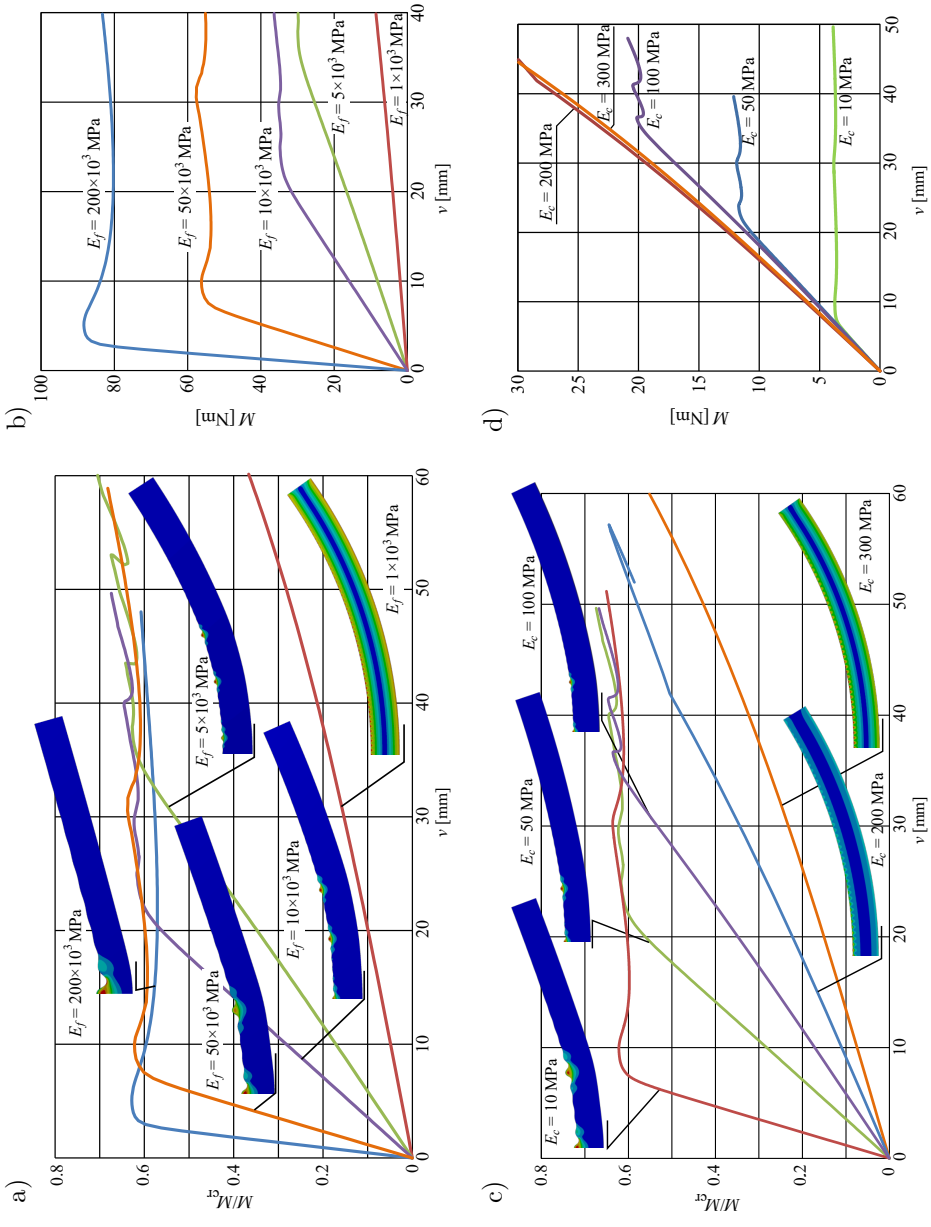

FIG. 9. Comparison of equilibrium paths and failure mode shapes for beams with different Young's moduli of the face (a), (b) and the core (c), (d).

This observation is valid for both series of models: the one in which the face varies and the one in which the core varies.

Aside from the buckling load, essential information is how the different models behave under the load and especially how the wrinkles form on the upper face. This is shown in the images added to the plots in Fig. 9a and Fig. 9c. In Fig. 9a, it is seen that for the face with the highest stiffness after the loss of stability, only one dimple forms and evolves with the increase of deflection. For lower values of Young's modulus, one dimple also appears, but with the increase of the deformation, additional dimples form, which is reflected in the path with additional peaks. In Fig. 9c, which corresponds to a fixed E_f and variable E_c, it is seen that the deformation has always the same form, two folds, the amplitude of which decreases with the increase of the core's stiffness. However, for $E_c = 200\,\text{MPa}$ and higher, the deformation has the form of regular wrinkles that diminish near the support.

3.4. Investigation of aluminium sandwich beams

The presented results are based on an arbitrarily selected model of the beam as well as properties of the material. To verify how the proposed models work, an additional study is provided further. The data used are based on the results of an experimental investigation carried out as a part of scientific grant no. N N502 080738, selected findings of which were presented in a monograph by Magnucki and Szyc [4]. The subject of the grant was aluminium sandwich beams with a metallic foam core, as shown in Fig. 10c. The beams consist of two solid pure aluminium faces and a core made of open-cell aluminium foam called Alporas®. All elements of the beam were glued together.

As an example, a beam with a width of 100 mm and a total thickness of 40 mm was chosen. The thickness of each face equals 1 mm. A four-point bending test was performed on the universal testing machine Zwick Z100, as shown in Fig. 10b to Fig. 10d. During the experimental test of the beam, the force was measured with a force transducer, and based on this value and the positions of the loading and support points, the bending moment was determined. The second measured value was the deflection at three points, recorded using inductive displacement transducers located in the central part of the beam, where pure bending conditions occurred. The displacement values at these three points were used as a guide to determine the curvature of the beam, assuming that cylindrical bending takes place. These two parameters, that is, the bending moment and curvature, were used to plot the results of experiments. The behaviour of the upper face of the beam was also monitored visually. However, the deformation had the character of small waves distributed randomly across the entire surface of the upper face. Therefore, it was not possible to determine

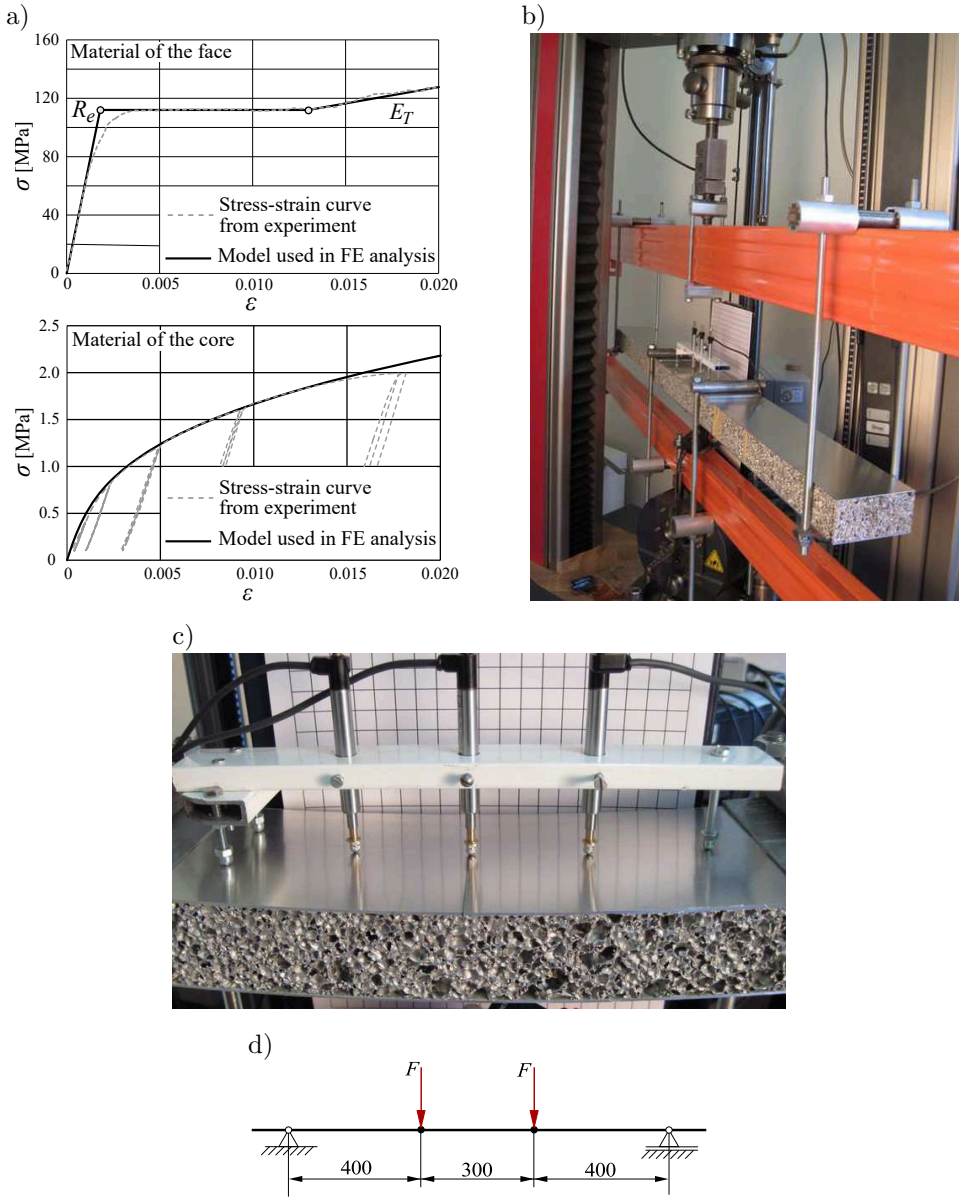

FIG. 10. Samples of structures used in experimental work: a) models of materials for FE analysis, b) and c) test stand, d) loading conditions.

critical changes in the global behaviour using this approach, unless there was a sudden decrease in stiffness, associated with local indentation resulting from delamination.

The material models of the faces and the core used to prepare the FE model are based on the results of static tests. In the case of solid aluminium used

to make the faces, a static tensile test was performed. In turn, to determine the mechanical properties of the foam, more convenient approach is to perform a static compression test. This way, the problem of clamping the specimen in the machine's jaw is eliminated. Furthermore, since the foam exhibits non-linear behaviour from the very beginning of the test, unloading stages were included in the loading process to form hysteresis loops. Based on these loops, Young's modulus can be determined. The results of both tests are shown in Fig. 10a as stress-strain curves marked with dashed lines. In contrast, the models used in the FE analyses are marked with solid lines. It was assumed that both materials behave in the same way under tensile and compressive stresses. The mechanical properties of the faces material are as follows: Young's modulus $E_f = 65.6 \times 10^3$ MPa, Poisson's ratio $\nu = 0.3$, yield point $R_e = 112$ MPa, and tangent modulus in the hardening region $E_T = 2.235 \times 10^3$ MPa. The stress-strain relationship for the core is described by Eq. (2.1) using the following parameters: $c = 400\,000$, $m = 1.01$, $E_c = 609$ MPa.

The actual beams were tested until failure. For this reason, a fully-plastic FE model was used to compare the results of the experiment (blue line) with the behaviour of the beam model (red line) shown in Fig. 11.

It can be seen that the initial stiffness of the beam and the FE model are identical. What is more important, the loss of stability takes place at the same value of the load equal to about 460 Nm. The differences appear after this point. On the curve corresponding to the experiment, a plateau region is seen, after which the strain-hardening phenomenon can be distinguished. In the case of the FE simulation, after the loss of stability, two regions of strain hardening are visible. The final shape mode of failure is similar for both analyses and has the form of a single dent near the mid-length, and it corresponds to about the same curvature of the beam and the FE model. Because, in the FE model, neither the separation of the layers nor the material interruption were taken into account, the core follows the face deformation during the whole analysis. In the actual beam, the failure has the character of face separation. As can be seen from images A and B in Fig. 11, after the loss of stability, plastic deformations start to grow according to a pattern corresponding to the initial imperfections. The deformation of the upper face is very small. Finally, a local fold appears in the location where the plastic strains are the highest.

The results of additional analyses are presented below, in which different FE models were used to understand how the material formulation may influence the behaviour of the beam model. The equilibrium paths obtained from all models presented in the previous section are compared in Fig. 12. The curve obtained in the experiment is marked with a blue line. It can be seen that the crucial parameter is the plasticity of the face. For both models with a plastic face, the limit load has the same value as the one from the experiment. If the

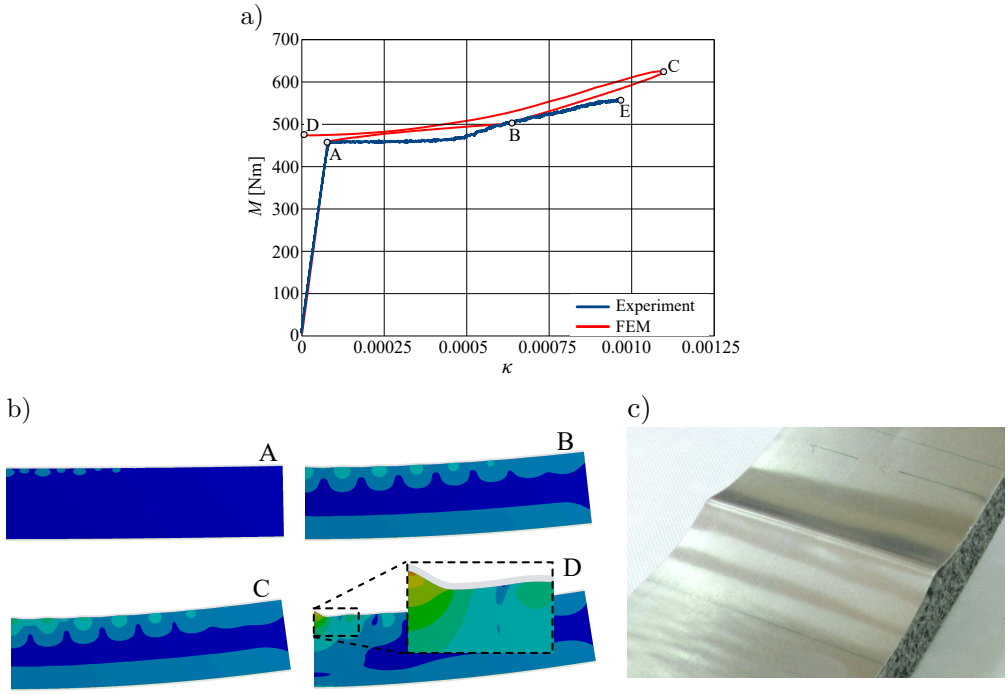

FIG. 11. Comparison of the results of the pure bending test: a) equilibrium paths, b) plastic strain in the FE model, c) failure of the tested beam.

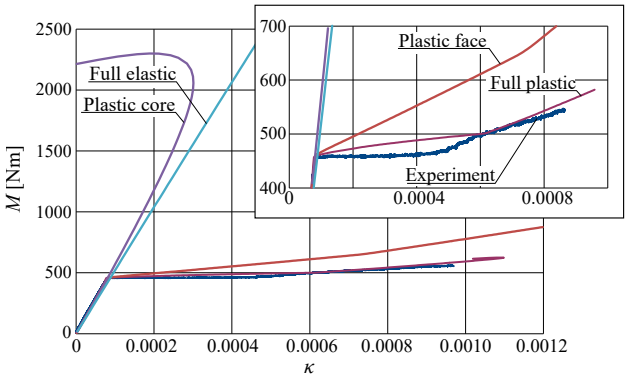

FIG. 12. Comparison of the behaviour of an actual beam and different FE models of the beam.

material of the face is an elastic one, the limit load increases up to 2.3 kNm for a plastic core. For the fully elastic model, the loss of stability is not observed. However, it should be noted that the value of the linear buckling load obtained in linear analysis equals about 7 kNm, which is 15 times higher than the value given by the plastic model and the experiment.

3.5. Influence of imperfection shape and magnitude

One of the crucial parameter influencing the post-buckling behaviour of the structure is the shape and magnitude of initial geometrical imperfections. These parameters may change both the value of the critical load as well as the shape that the structure will take after the loss of stability. The research on this subject is performed on an aluminium beam of the same parameters as in the previous section, with the difference that the width of the beam equals 50 mm. Four different shapes of imperfections are examined corresponding to the 1st, 2nd, and 4th buckling modes, and the combination of these three. The third mode was omitted to avoid its interference with the first mode, since it may result in a large peak at the mid-span of the beam. The buckling modes are provided in Fig. 13a.

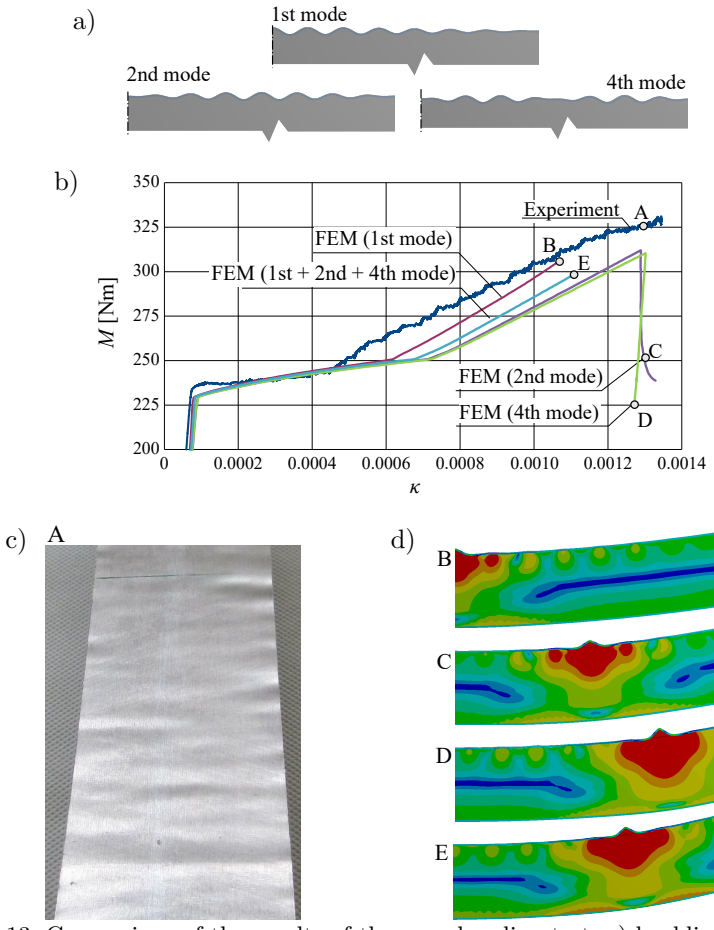

Fig. 13. Comparison of the results of the pure bending test: a) buckling modes, b) equilibrium paths, c) failure of the tested beam, d) elastic strain in the FE model.

They all have the shape of sine waves, which in the case of the 1st mode have a maximum at the mid-length and fade towards the support. In the case of the 2nd mode, the maximum is in the middle of the half-beam, fading towards the mid-length and the support. The last 4th mode is irregular. Since in this subsection the influence of the imperfection on the buckling behaviour is the main goal, a higher amplitude than before is assumed, that is, 0.1 mm. In the case of a combination of three different modes, each mode was introduced with a value equal to 0.0333 mm.

The results obtained from the FE analyses (fully plastic model) are presented in the form of equilibrium paths in Fig. 13b and compared with the plot obtained from the experiment. The comparison looks similar to that for the wider beam presented before. The initial stiffness of the FE model and the actual beam is the same. A small discrepancy, about 3 %, between the value of load at which the loss of stability takes place is visible. For the beam from experiment, the value is slightly higher, equal to 235 Nm, and after that point an almost flat region can be distinguished. For the FE model, a strain-hardening region can be seen. In general, the shape of the imperfection does not influence the post-buckling behaviour of the model. When the curves from Fig. 13b are compared, the difference appears only in the moment at which the local fold starts to form. The slope of the last part of all paths is comparable. The shape of the failure mode is also the same, with the difference that the location of the final single dent is determined by the initial imperfection. The failure of the actual beam is shown in Fig. 13c. Here, a number of plastic folds are spread on the whole upper face, without a single clearly visible dent.

An exemplary imperfection sensitivity analysis is performed for the second buckling mode. The magnitudes of imperfection are equal to (0.01, 0.05, 0.2, 0.5 and 1.0) mm. Also, in this analysis, the equilibrium paths are generated with the use of the FEM and are presented in Fig. 14. For small imperfections, the

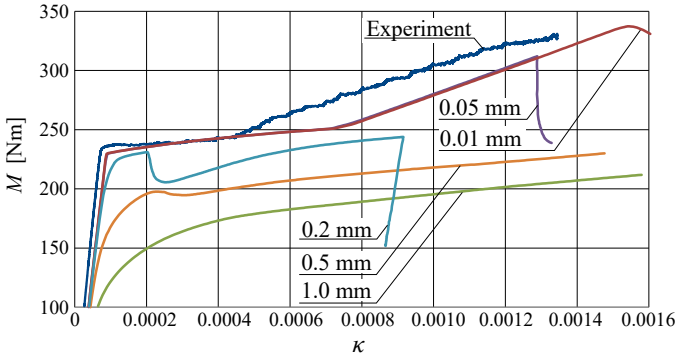

FIG. 14. Influence of the imperfection magnitude (2nd buckling mode) on the post-buckling behaviour of the model.

path looks the same, except for the point where it collapses. If the imperfection is higher, a sudden drop of the path can be observed, as in the case of the value equal to 0.2 mm. For the highest analysed imperfection, the path is smooth during the whole process of the beam deformation.

4. Conclusions

When analysing the results presented above, the first thing that comes to mind is that the phenomenon of local loss of stability of a sandwich beam is strongly influenced by the mechanical properties of the materials of the particular layers. By comparing the results of analyses for four different models of the beam, it can be seen that in the pre-buckling linear range there is no difference in the behaviour. Only elastic deformation appears, and the stiffness of all models is the same – the same slope of the initial part of the equilibrium paths (see Fig. 7a). This means that for deflection analysis in the small deformation range, any model should work correctly.

When it comes to the control of the buckling shape, it can be seen that a stiffer face leads to a small number of waves with large amplitude (Fig. 8a). On the contrary, by increasing the core stiffness, a large number of waves with small amplitude can be obtained (Fig. 8b). However, if the plastic behaviour of the material is taken into account, the deformation in the post-buckling range always takes the form of local folds, the number of which depends on the material and the magnitude of deformation.

An important information is that the stiffness of the beam can be barely increased by increasing Young's modulus of the core. From the example presented in Fig. 9d, it is seen that increasing the value from 10 to 200 MPa increases the stiffness of the model by about 22 %.

Since the present investigation was focused on the response of beams with different models of materials during loss of stability, only one type of initial geometrical imperfections was considered, namely that corresponding to the eigenmode obtained in the linear buckling analysis. However, further investigations are planned in which natural imperfections can be incorporated based on measurements of actual specimens. Also, other types of imperfections, such as delamination or voids, can be crucial, especially for new complex materials such as composites or foams.

It should be noted that the model presented in this paper is 2D. As a consequence, the wrinkles or folds that appear after the buckling are assumed to spread through the entire depth of the beam. As it was shown in Fig. 13c, in an actual beam, folds of various sizes spread across the entire upper face which, among others, can be the result of discontinuities of the foamed core. Such a simplified model may be a source of discrepancies between the results obtained with

the two methods; however, when these results are compared, the values analysed in the investigation are similar and the discrepancies are acceptable.

Fundings

This work was developed based on the statutory activity of the Poznan University of Technology (grant of the Ministry of Science and Higher Education in Poland no. 0612/SBAD/3628).

Conflict of interest

The authors declare that there are no known competing financial interests or personal relationships that could have influenced the work described in this paper.

Authors' contributions

Paweł Jasion was responsible for the research concept and design, theory development, calculations and simulations, and preparation of the original draft. Iwona Wstawska was responsible for data collection and analysis, measurements and experiments, calculations and simulations, and manuscript review and editing. Kamil Kołodziński was responsible for formal analysis, interpretation of the results, and preparation of the conclusions. All authors reviewed and approved the final manuscript.

References

1. Hadi B.K., Wrinkling of sandwich column: Comparison between finite element analysis and analytical solutions, *Composite Structures*, **53**(4): 477–482, 2001, https://doi.org/10.1016/S0263-8223(01)00060-5.

2. Jasion P., Magnucki K., Buckling-wrinkling of a face of sandwich beam under pure bending [in Polish: Wyboczenie-zmarszczenie okładziny belki trójwarstwowej przy czystym zginaniu], *Modelowanie Inżynierskie*, **10**(41): 151–156, 2011.

3. Jasion P., Magnucki K., Global buckling of a sandwich column with metal foam core, *Journal of Sandwich Structures and Materials*, **15**(6): 718–732, 2013, https://doi.org/10.1177/1099636213499339.

4. Magnucki K., Szyc W., *Strength and Stability of Sandwich Beams and Plates with Aluminium Foam Core* [in Polish: Wytrzymałość i Stateczność Belek i Płyt Trójwarstwowych z Rdzeniem z Pianki Aluminiowej], Wydawnictwo Politechniki Poznańskiej, Poznań, 2012.

5. Jasion P., Magnucki K., Face wrinkling of sandwich beams under pure bending, *Journal of Theoretical and Applied Mechanics*, **50**(4): 933–941, 2012.

6. Stiftinger M.A., Rammerstorfer F.G., Face layer wrinkling in sandwich shells – Theoretical and experimental investigations, *Thin-Walled Structures*, **29**(1–4): 113–127, 1997, https://doi.org/10.1016/S0263-8231(97)00018-9.

7. Sjölander J., Hallander P., Åkermo M., Forming induced wrinkling of composite laminates: A numerical study on wrinkling mechanisms, *Composites Part A: Applied Science and Manufacturing*, **81**: 41–51, 2016, https://doi.org/10.1016/j.compositesa.2015.10.012.

8. Sudhakar V., Vijayaraju K., Gopalakrishnan S., Development of a new finite element for the analysis of sandwich beams with soft core, *Journal of Sandwich Structures and Materials*, **12**(6): 649–683, 2010, https://doi.org/10.1177/1099636210363340.

9. Birman V., Bert C.W., Wrinkling of composite-facing sandwich panels under biaxial loading, *Journal of Sandwich Structures and Materials*, **6**(3): 217–237, 2004, https://doi.org/ 10.1177/1099636204033643.

10. El-Sayed S., Sridharan S., Imperfection-sensitivity of integral and debonded sandwich beams under compression, *Journal of Sandwich Structures and Materials*, **4**(1): 49–69, 2002, https://doi.org/10.1177/1099636202004001223.

11. Lolive É., Berthelot J.-M., Non-linear behaviour of foam cores and sandwich materials, part 2: Indentation and three-point bending, *Journal of Sandwich Structures and Materials*, **4**(4): 297–352, 2002, https://doi.org/10.1106/109963602024046.

12. Frostig Y., Birman V., Kardomateas G.A., Non-linear wrinkling of a sandwich panel with functionally graded core – Extended high-order approach, *International Journal of Solids and Structures*, **148–149**: 122–139, 2018, https://doi.org/10.1016/j.ijsolstr.2018.02.023.

13. Vescovini R., D'Ottavio M., Dozio L., Polit O., Buckling and wrinkling of anisotropic sandwich plates, *International Journal of Engineering Science*, **130**: 136–156, 2018, https://doi.org/10.1016/j.ijengsci.2018.05.010.

14. Mhada K., Bourihane O., A multi-scale model for global buckling and local wrinkling interaction with application to sandwich beams, *Structures*, **32**: 1398–1407, 2021, https://doi.org/10.1016/j.istruc.2021.03.042.

15. Cao P., Niu K., New unified model of composite sandwich panels/beams buckling introducing interlayer shear effects, *Composite Structures*, **252**: 112722, 2020, https://doi.org/10.1016/j.compstruct.2020.112722.

16. Karamanli A., Aydogdu M., Buckling of laminated composite and sandwich beams due to axially varying in-plane loads, *Composite Structures*, **210**: 391–408, 2019, https://doi.org/10.1016/j.compstruct.2018.11.067.

17. Liu J., He B., Ye W., Yang F., High performance model for buckling of functionally graded sandwich beams using a new semi-analytical method, *Composite Structures*, **262**: 113614, 2021, https://doi.org/10.1016/j.compstruct.2021.113614.

18. Wang T., Liu F., Fu C., Zhang X., Wang K., Xu F., Curvature tunes wrinkling in shells, *International Journal of Engineering Science*, **164**: 103490, 2021, https://doi.org/10.1016/j.ijengsci.2021.103490.

19. Su W., Liu S., A couple-stress model to predict the wrinkling stress of sandwich panels with foam cores, *Composite Structures*, **268**: 113978, 2021, https://doi.org/10.1016/j.compstruct.2021.113978.

20. Li H., Sun H., Liu H., Liu N., Loading conditions constrained wrinkling behaviors of thin-walled sheet/tube parts during metal forming, *Journal of Materials Processing Technology*, **296**: 117199, 2021, https://doi.org/10.1016/j.jmatprotec.2021.117199.

21. Hu H., Cao D., Cao Z., Li S., Experimental and numerical investigations of wrinkle effect on failure behavior of curved composite laminates, *Composite Structures*, **261**: 113541, 2021, https://doi.org/10.1016/j.compstruct.2021.113541.

22. Huang W., Yan W., Xu R., Huang Q., Yang J., Trochu F., Hu H., Wrinkling analysis of circular membranes by a Fourier based reduced model, *Thin-Walled Structures*, **161**: 107512, 2021, https://doi.org/10.1016/j.tws.2021.107512.

23. Leotoing L., Drapier S., Vautrin A., Using new closed-form solutions to set up design rules and numerical investigations for global and local buckling of sandwich beams, *Journal of Sandwich Structures and Materials*, **6**(3): 263–289, 2004, https://doi.org/10.1177/1099636204034632.

24. Léotoing L., Drapier S., Vautrin A., Nonlinear interaction of geometrical and material properties in sandwich beam instabilities, *International Journal of Solids and Structures*, **39**(13–14): 3717–3739, 2002, https://doi.org/10.1016/S0020-7683(02)00181-6.

25. Fagerberg L., Zenkert D., Imperfection-induced wrinkling material failure in sandwich panels, *Journal of Sandwich Structures and Materials*, **7**(3): 195–219, 2005, https://doi.org/10.1177/1099636205048526.

26. Douville M.-A., Le Grognec P., Exact analytical solutions for the local and global buckling of sandwich beam-columns under various loadings, *International Journal of Solids and Structures*, **50**(16–17): 2597–2609, 2013, https://doi.org/10.1016/j.ijsolstr.2013.04.013.

27. Ramberg W., Osgood W.R., Description of stress-strain curves by three parameters, Technical Note no. 902, *NACA Technical Notes*, Washington, 1943.

Received July 10, 2025; revised November 20, 2025; accepted December 3, 2025; available online December 11, 2025; version of record June 3, 2026; published issue XXXX.